

Suppression of lncRNA-MALAT1 activity ameliorates femoral head necrosis by modulating mTOR signaling

Luyao Ma¹, Jian Gao²

¹Department of Orthopaedics, Second Hospital of Shanxi Medical University, Taiyuan, Shanxi, China

²Second Clinical Medical College, Shanxi Medical University, Taiyuan, Shanxi, China

Submitted: 9 September 2019; **Accepted:** 19 December 2019

Online publication: 2 February 2020

Arch Med Sci 2024; 20 (2): 612–617

DOI: <https://doi.org/10.5114/aoms.2020.92829>

Copyright © 2020 Termedia & Banach

Corresponding author:

Luyao Ma
Department of Orthopaedics
Second Hospital of
Shanxi Medical University
382 Wuyi Road
Taiyuan
Shanxi 030001, China
E-mail: UriahHopkinsmhr@yahoo.com

Abstract

Introduction: Avascular necrosis of the femoral head (ANFH) is one of the most complicated bone disorders; management remains challenging. We evaluated the effect of lncRNA-MALAT1 suppression on ANFH rats.

Material and methods: Dexamethasone was injected intravenously at 0.5 mg/kg daily for 30 days to induce ANFH; an lncRNA-MALAT1 inhibitor group received the inhibitor for the entire 30 days. lncRNA-MALAT1 suppression was evaluated by measuring blood hexosamine and hydroxyproline levels, and that of circulating endothelial progenitor cells (EPCs). Changes in femoral head bone ultrastructure were assessed via transmission electron microscopy and magnetic resonance imaging (MRI). We used reverse transcription polymerase chain reaction (RT-PCR) and Western blotting to measure gene and protein expression levels in femoral head tissue.

Results: The blood hexosamine level rose and that of hydroxyproline fell in the lncRNA-MALAT1 inhibitor group compared to the ANFH group. lncRNA-MALAT1 suppression increased the level of circulating EPCs. Ultrastructural changes in the femoral bone head were alleviated by the lncRNA-MALAT1 inhibitor. lncRNA-MALAT1 suppression lowered the levels of AMPK, mTOR, and Beclin-1 in rat tissue homogenates.

Conclusions: lncRNA-MALAT1 suppression attenuated dexamethasone-induced femoral head necrosis by regulating AMPK/mTOR/Beclin-1 signaling.

Key words: lncRNA-MALAT1, femoral head necrosis, dexamethasone, hexosamine.

Introduction

Orthopedic specialists find it very difficult to manage avascular necrosis of the femoral head (ANFH), which is associated with reduced blood supply to bony tissue, femoral bone destruction, and pain [1]. China has approximately 200,000 such patients [2]. Subchondral bone becomes damaged and the bone marrow ischemic [3]. Several non-traumatic conditions contribute to bone destruction, including wounds, chronic pancreatitis, systemic lupus erythematosus, and excessive intake of alcohol or corticosteroids [4] (the latter are commonly used to manage several disorders). Corticosteroids reduce blood flow and increase intraosseous pressure by regulating bone marrow adipogenesis [5]. Endothelial cell (EDC) integrity is also compromised, triggering femoral head necrosis [6]. Corticosteroids affect the osteoclast/osteoblast balance regulated by several molecular pathways including autophagy [7]. lncRNAs control

several physiological functions including those of osteocytes [8]. lncRNA-MALAT1 regulates the development of squamous cell carcinoma, lung cancer, and glioma [9], and enhances osteosarcoma proliferation. lncRNA-MALAT1 inhibits apoptosis and promotes osteoclast function by attenuating DLL3 gene expression and modulating Notch signaling; osteoporosis may then develop [10, 11]. lncRNA-MALAT1 suppression protects against lung injury by reducing IL-8 levels [12].

Here, we evaluated the effect of lncRNA-MALAT1 suppression on ANFH.

Material and methods

Animals

Male Sprague-Dawley rats (150–200 g) were kept under a 12-h/12-h light/dark cycle at 60 ±5% relative humidity and 24 ±3°C. All animal protocols were approved by the animal ethics committee of the Second Hospital of Shanxi Medical University, China (approval no. IAEC/SH-SMU/2017/08). All protocols adhered to the draft Animal Protection Law of the People's Republic of China 2009.

Chemicals

The lncRNA-MALAT1 inhibitor was purchased from Youbio Biological Technology Co. Ltd., Hunan, China. Dexamethasone was from Sigma-Aldrich (St. Louis, MO, USA). Primary antibodies used for Western blotting were from Cell Signaling Technology (Beverly, MA, USA) and secondary antibodies from Tianjin Sungene Biotech (Tianjin, China).

Experimental

ANFH was induced in rats as previously reported [13]. Dexamethasone was injected intravenously at 0.5 mg/kg daily for 30 days. The animals were divided into three groups: sham; ANFH; and lncRNA-MALAT1 inhibitor groups. The latter group received the lncRNA-MALAT1 inhibitor intraperitoneally 30 min prior to the dexamethasone injection on each of the 30 days. All rats were then sacrificed, bone marrow EPCs were isolated, and the femoral heads were prepared.

Hexosamine and hydroxyproline assays

Blood was drawn from the retro-orbital plexus prior to sacrifice and serum was obtained by centrifugation at 2,000 RPM for 10 min. Hexosamine and hydroxyproline levels were estimated as described previously [14].

Femoral head ultrastructure evaluation

Femoral heads were fixed for 24 h in glutaraldehyde (2% w/v) and washed with PBS (0.1 M

NaCl). Nitric acid solutions of 2, 4, and 5% (v/v) were used to decalcify the tissues, which were then dehydrated with ethanol, embedded in epoxy resin, sectioned into ultrathin slices (75-nm-thick), stained with uranyl acetate and lead citrate, and examined using a JEM-1200EX transmission electron microscope.

Magnetic resonance imaging (MRI)

ANFH was diagnosed and staged via MRI of the bilateral proximal femora using a 3.0-T superconducting platform. The short tau inversion recovery (STIR) imaging parameters were: repetition time (TR) = 6,200 ms; echo time (TE) = 30 ms; FOV = 16 × 16; matrix = 256 × 146; and excitation flip angle = 90°. A high STIR signal indicated fat; computed tomography (CT) was used to determine bone mineral density (BMD) and femoral head osteonecrosis.

EPC assay

Flow cytometry was used to measure blood EPC levels. Single-cell suspensions were prepared by centrifuging homogenized blood for 5 min at 1,500 RPM; the pellet was resuspended in PBS and anti-Flk-1 and -Sca-1 antibodies were added, followed by incubation for 1 h. Sca-1/Flk-1 doubly positive mononuclear cells were considered to be EPCs.

Western blotting

Total proteins were extracted from bone-marrow-derived EPCs (BMD-EPCs) into NP40 protein lysis buffer and assayed using the DC Protein Assay. Proteins were separated via sodium dodecyl sulfate (SDS)-polyacrylamide gel (10%) electrophoresis and transferred to polyvinylidene difluoride membranes. The membranes were blocked overnight in 5% (w/v) fresh non-fat dry milk; incubated at 4°C overnight with primary antibodies against p-mTOR, mTOR, p-AMPK, AMPK, Beclin-1 and β-actin; washed; and incubated with secondary antibodies for 60 min at room temperature. Chemiluminescence was used to enhance the blot and ImageLab software was used to perform densitometric analysis.

RT-PCR

BMD-EPC total RNA was isolated using Trizol reagent and the RNA was reverse-transcribed with the aid of a RevertAid First Strand cDNA Synthesis Kit. Primers (see below) were added and an RT 2 SYBR Green Master Kit was used to determine gene expression levels employing the Quantitative SYBR Green PCR assay. The program used was 98°C for 2 min followed by 25–40 cycles of 98°C

for 10 s, 55°C for 5 s, and 72°C for 20 s. mRNA expression levels were calculated using standard curves generated by plotting the quantification cycle (Cq) against the log of the total cDNA level. Relative gene expression levels were determined using the $2^{-\Delta\Delta Cq}$ method.

Primer Forward
 AMPK 5'-AGGAAGAATCCTGTGACAAGCAC-3'
 Reverse 5'-CCGATCTCTGTGGAGTAGCAGT-3'
 Primer Forward
 mTOR 5'-CTCAACATCGAGCATCGCATCATG-3
 Reverse 5'-ACCAGAAAGGGCACCAGCCAATATAG-3
 Primer Forward
 CaMKK β 5'-CGAUCGUCAUCUCUGGUUAdTdT-3'
 Reverse 5'-UAACCAGAGAUGACGAUCGdTdT-3'
 Primer Forward
 GAPDH 5'-ACCACAGTCCATGCCATCAC-3'
 Reverse 5'-TCCACCACCTGTTGCTG-3'

Statistical analysis

All data are expressed as means \pm SEMs ($n = 10$) and were compared using one-way analysis of variance (ANOVA) with Dunnett's *post hoc* test us-

ing GraphPad Prism (ver. 6.1; San Diego, CA, USA). *P*-values < 0.05 were considered to indicate statistical significance.

Results

LncRNA-MALAT1 suppression affected hexosamine and hydroxyproline levels

The effects of LncRNA-MALAT1 inhibition on the serum concentrations of hexosamine and hydroxyproline in ANFH rats are shown in Figure 1. The hexosamine level fell and the hydroxyproline level increased, compared to the sham-operated group; the hexosamine/hydroxyproline molar ratio was lower in the former group. However, inhibition of LncRNA-MALAT1 action ameliorated these changes.

Effect of LncRNA-MALAT1 suppression on femoral bone ultrastructure

Transmission electron microscopy (Figure 2) showed that the femoral head ultrastructure of the sham-operated group was normal. In the ANFH group, reductions in the levels of endoplasmic reticulum and mitochondrial cristae were apparent, and the cells lacked chromatin, accom-

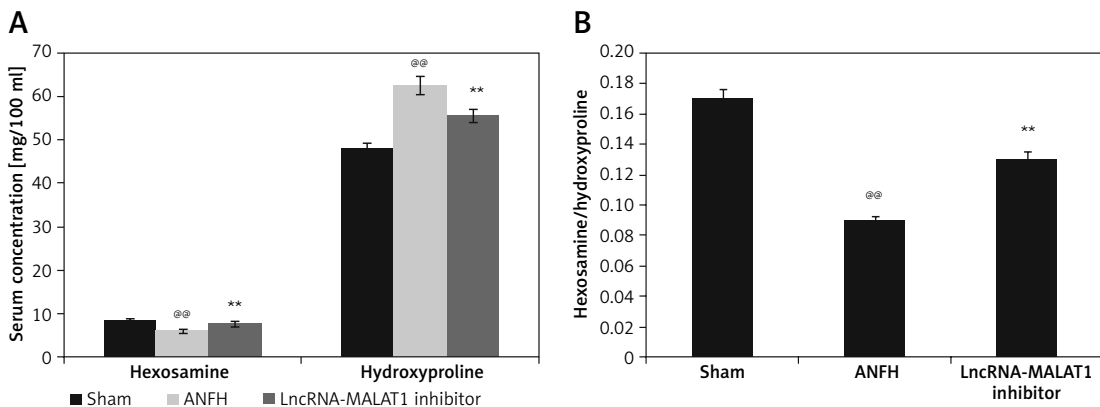


Figure 1. Effects of LncRNA-MALAT1 inhibition on the serum concentrations of hexosamine and hydroxyproline in ANFH rats. Means \pm SEMs ($n = 10$). $^{@@}p < 0.01$ compared to the sham-operated group; $^{**}p < 0.01$ compared to the ANFH group

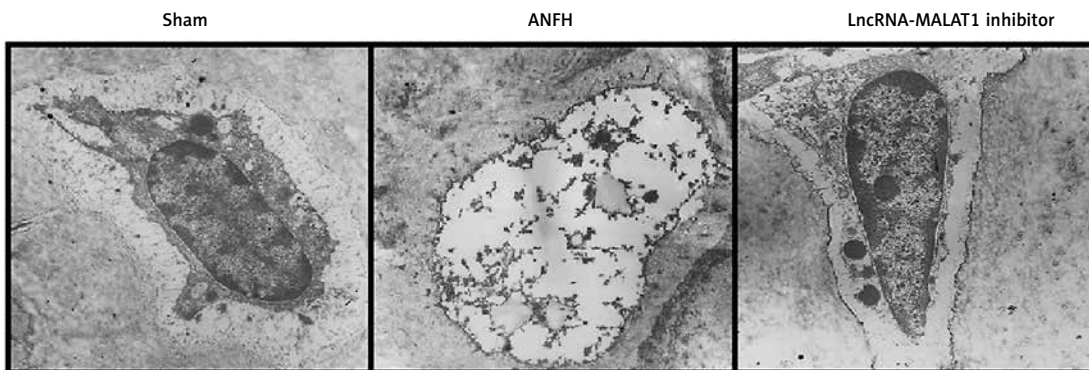


Figure 2. Effects of LncRNA-MALAT1 inhibition on femoral head ultrastructure in ANFH rats as revealed by transmission electron microscopy

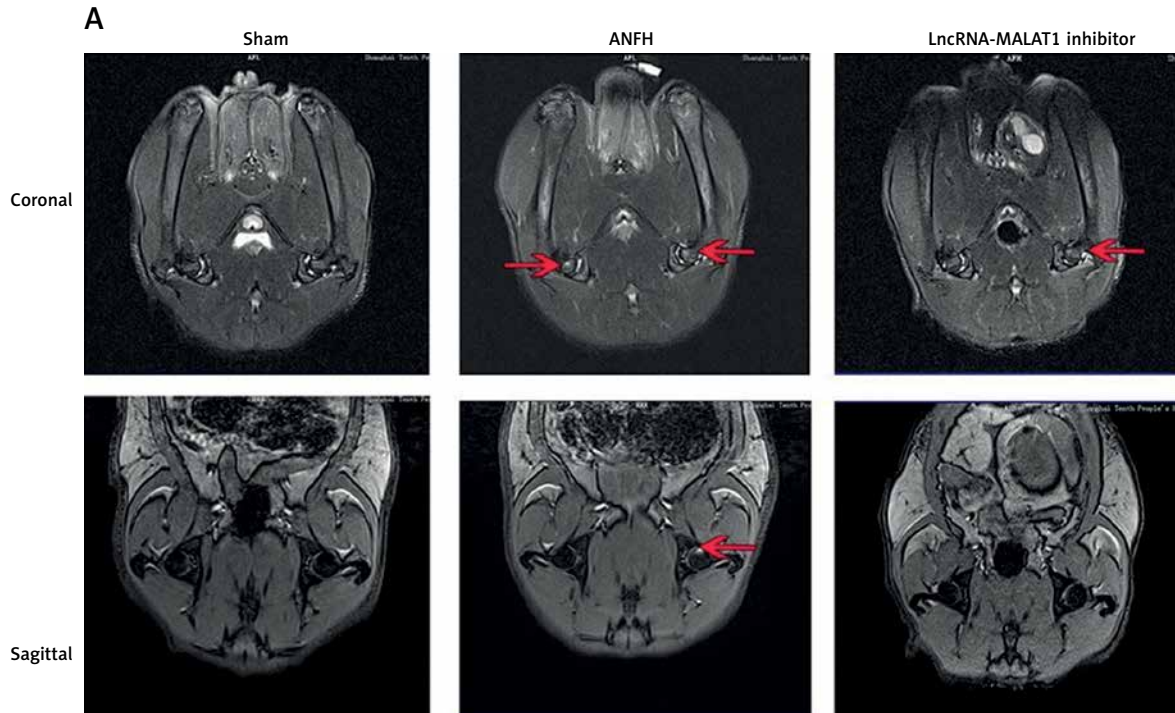


Figure 3. Effects of lncRNA-MALAT1 inhibition on MRI images of the femoral head in ANFH rats. **A** – STIR image, **B** – Bone mineral density. Means \pm SEMs ($n = 10$); $^{\circ\circ}p < 0.01$ compared to the sham-operated group; $^{**}p < 0.01$ compared to the ANFH group

panied by karyolysis, karyorrhexis, pyknosis, and vacuolization. Suppression of lncRNA-MALAT1 action attenuated femoral head necrosis.

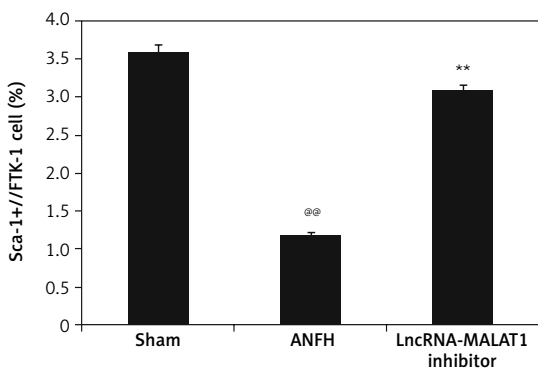


Figure 4. Effect of lncRNA-MALAT1 inhibition on the proportion of circulating EPCs in the blood of ANFH rats. Means \pm SEMs ($n = 10$); $^{\circ\circ}p < 0.01$ compared to the sham-operated group; $^{**}p < 0.01$ compared to the ANFH group

Effect of lncRNA-MALAT1 suppression on MRI data

Figure 3 shows that the STIR femoral head signals were of moderate intensity and normal homogeneity in the sham-operated group. In the ANFH group, the signals were of high intensity, accompanied by abnormal myxoid or lipidoidal changes, but this was not the case in the group given the lncRNA-MALAT1 inhibitor. The BMD was significantly reduced ($p < 0.01$) in the ANFH compared to the sham-operated, but not the lncRNA-MALAT1 inhibitor-treated, group.

Effect of lncRNA-MALAT1 suppression on the quantity of circulating EPCs

Flow cytometry (Figure 4) showed that the proportion of Sca-1/Flk-1-positive cells (EPCs) was significantly lower ($p < 0.01$) in the ANFH group than in the sham-operated group, but this was not the case in the group given the lncRNA-MALAT1 inhibitor.

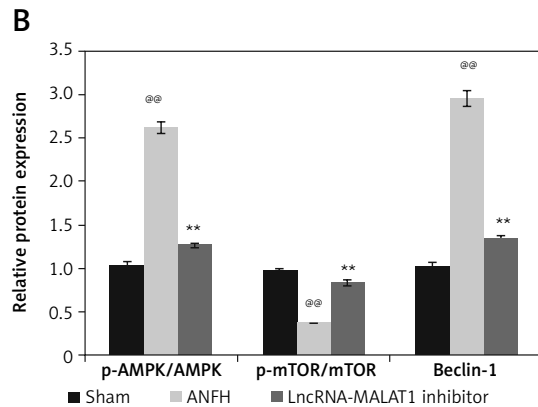
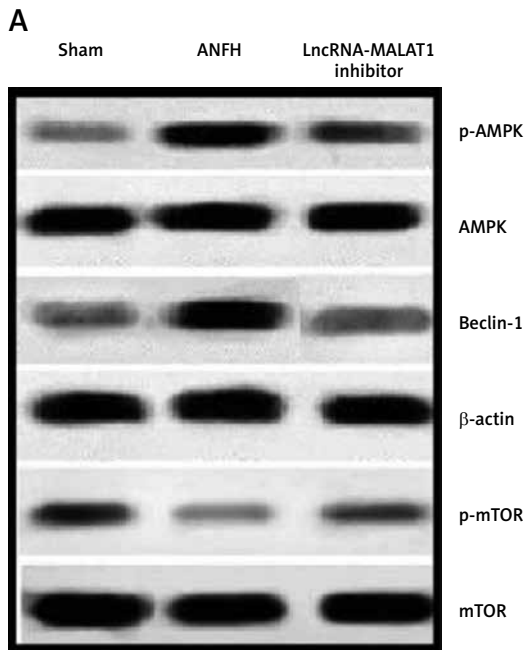


Figure 5. Effects of lncRNA-MALAT1 inhibition on expression of AMPK, mTOR, and Beclin-1 protein in femoral head tissue of ANFH rats. Means \pm SEMs ($n = 10$); @@ $p < 0.01$ compared to the sham-operated group; ** $p < 0.01$ compared to the ANFH group

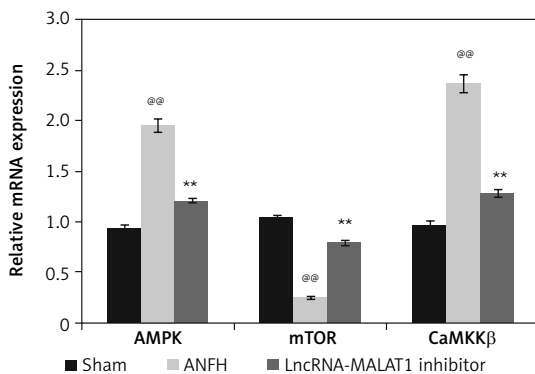


Figure 6. Effects of lncRNA-MALAT1 inhibition on expression levels of mRNAs encoding AMPK, mTOR, and CaMKK β in femoral head tissue of ANFH rats. Means \pm SEMs ($n = 10$); @@ $p < 0.01$ compared to the sham-operated group; ** $p < 0.01$ compared to the ANFH group

Effect of lncRNA-MALAT1 suppression on expression levels of mTOR, AMPK, and Beclin-1

In ANFH rats, mTOR and Beclin-1 levels in the femoral head were enhanced, and that of AMPK reduced, compared to sham-operated rats (Figure 5). The lncRNA-MALAT1 inhibitor significantly reduced mTOR and Beclin-1 protein expression ($p < 0.01$) and enhanced AMPK expression, compared to the ANFH group.

Effect of lncRNA-MALAT1 suppression on levels of mRNAs encoding AMPK, mTOR, and CaMKK β

We explored how lncRNA-MALAT1 inhibition affected expression of mRNAs encoding AMPK,

mTOR, and CaMKK β in the femoral head tissue of ANFH rats (Figure 6). Compared to sham-operated rats, the levels of mRNAs encoding AMPK and CaMKK β were enhanced and the levels of mRNAs encoding mTOR reduced in the ANFH group. In the lncRNA-MALAT1 inhibitor group, the mRNA expression levels did not change.

Discussion

Either ischemia or corticosteroids may trigger ANFH, treatment of which remains challenging; we evaluated the effects of lncRNA-MALAT1 suppression on rat ANFH by estimating blood hexosamine and hydroxyproline levels, and circulating EPC numbers. We used transmission electron microscopy and MRI to assess changes in femoral head bone ultrastructure. RT-PCR and Western blotting were employed to measure gene and protein expression levels in femoral head tissue.

Corticosteroids increase the risk of ANFH by enhancing intracortical pressure, changing lipid metabolism, and triggering intravascular coagulation [15]. Vasculitis of femoral head tissue develops, accompanied by the appearance of anti-phospholipid antibodies [16]. We induced ANFH by administering a corticosteroid to rats. Blood hexosamine and hydroxyproline levels are major indicators of bone necrosis [17]. Hexosamine is a mucopolysaccharide, the synthesis of which is reduced when osteoclastic resorption is promoted and osteoblastic formation inhibited [18]. Hydroxyproline is present in collagen, the major component of bone [19]. The levels of these materials, and their molar ratio, were altered in the

blood of ANFH rats [20]. In the presence of the lncRNA-MALAT1 inhibitor, such changes were not apparent; normal femoral head BMD and ultra-structure were maintained.

Reduced EPC numbers/functionality increases the risk of ANFH [21]. It was found that EPC levels were significantly ($p < 0.01$) reduced in the blood of ANFH rats and suppression of lncRNA-MALAT1 increased EPC levels. Autophagy protects cells by inhibiting mTOR [22]. Data of the investigation reveal that suppression of lncRNA-MALAT1 inhibition significantly ($p < 0.01$) reduced mTOR expression compared to that of the ANFH group.

In conclusion, suppression of lncRNA-MALAT1 attenuated necrosis of the femoral head in dexamethasone-treated induced ANFH rats by regulating AMPK/mTOR/Beclin-1 signaling. Clinical evaluation is required; we used only a rat model.

Acknowledgments

All authors thank the Doctor Foundation of the Second Hospital of Shanxi Medical University, China (grant no. 201701-18) for supporting our work.

Conflict of interest

The authors declare no conflict of interest.

References

- Fondi C, Franchi A. Definition of bone necrosis by the pathologist. *Clin Cases Miner Bone Metab* 2007; 4: 21-6.
- Li HQ, Wu L, Jia ZP, Zhang XF, Sheng L. Investigation on mental health state of 37 patients of femoral head. *Zhonghua Liu Xing Bing Xue Za Zhi* 2012; 33: 1223.
- Stewart HL, Kawcak CE. The importance of subchondral bone in the pathophysiology of osteoarthritis. *Front Vet Sci* 2018; 5: 178.
- Goulden MR. The pain of chronic pancreatitis: a persistent clinical challenge. *Br J Pain* 2013; 7: 8-22.
- Wu B, Dong Z, Li S, Song H. Steroid-induced ischemic bone necrosis of femoral head: treatment strategies. *Pak J Med Sci* 2015; 31: 471-6.
- Pouya F, Kerachian MA. Avascular necrosis of the femoral head: are any genes involved? *Arch Bone Jt Surg* 2015; 3: 14-55.
- Yang DH, Yang MY. The role of macrophages in the pathogenesis of osteoporosis. *Int J Mol Sci* 2019; 20: E2093.
- Tye CE, Gordon JA, Martin-Buley LA, Stein JL, Lian JB, Stein GS. Could lncRNAs be the missing links in control of mesenchymal stem cell differentiation? *J Cell Physiol* 2015; 230: 526-34.
- Sun Y, Ma L. New insights into long non-coding RNA MALAT1 in cancer and metastasis. *Cancers (Basel)* 2019; 11: 216.
- Wang Y, Luo TB, Liu L, Cui ZQ. lncRNA LINC00311 promotes the proliferation and differentiation of osteoclasts in osteoporotic rats through the Notch signaling pathway by targeting DLL3. *Cell Physiol Biochem* 2018; 47: 2291-306.
- Zheng S, Wang YB, Yang YL, et al. lncRNA MALAT1 inhibits osteogenic differentiation of mesenchymal stem cells in osteoporosis rats through MAPK signaling pathway. *Eur Rev Med Pharmacol Sci* 2019; 23: 4609-17.
- Wei L, Li J, Han Z, Chen Z, Zhang Q. Silencing of lncRNA MALAT1 prevents inflammatory injury after lung transplant ischemia-reperfusion by downregulation of IL-8 via p300. *Mol Ther Nucleic Acids* 2019; 18: 285-97.
- Song Q, Ni J, Jiang H, Shi Z. Sildenafil improves blood perfusion in steroid-induced avascular necrosis of femoral head in rabbits via a protein kinase G-dependent mechanism. *Acta Orthop Traumatol Turc* 2017; 51: 398-403.
- Dwivedi D, Dwivedi M, Malviya S, Singh V. Evaluation of wound healing, anti-microbial and antioxidant potential of *Pongamia pinnata* in Wistar rats. *J Tradit Complement Med* 2016; 7: 79-85.
- Gold EW, Fox OD, Edgar PR. The effect of long term corticosteroid administration on lipid and prostaglandin levels. *J Steroid Biochem* 1978; 9: 313-6.
- Adikari M, Gunawardane A, Illangantilaka S, Atukorale H, Rubasinghe J. A case of systemic lupus erythematosus presenting as bilateral avascular necrosis of femur. *BMC Res Notes* 2016; 9: 392.
- Zhang M, Hu X. Mechanism of chlorogenic acid treatment on femoral head necrosis and its protection of osteoblasts. *Biomed Rep* 2016; 5: 57-62.
- Weinstein RS, Jilka RL, Parfitt AM, Manolagas SC. Inhibition of osteoblastogenesis and promotion of apoptosis of osteoblasts and osteocytes by glucocorticoids. Potential mechanisms of their deleterious effects on bone. *J Clin Invest* 1998; 102: 274-82.
- Lodish H, Berk A, Zipursky SL, et al. *Molecular Cell Biology*. 4th edition. W.H. Freeman, New York 2000. Section 22.3, Collagen: The Fibrous Proteins of the Matrix.
- Shi B, Li G, Wang P, et al. Effect of antler extract on corticosteroid-induced avascular necrosis of the femoral head in rats. *J Ethnopharmacol* 2010; 127: 124-9.
- Feng Y, Yang SH, Xiao BJ, et al. Decreases in the number and function of circulation endothelial progenitor cells in patients with avascular necrosis of the femoral head. *Bone* 2010; 46: 32-40.
- Zhu Z, Yang C, Iyaswamy A, et al. Balancing mTOR signaling and autophagy in the treatment of Parkinson's Disease. *Int J Mol Sci* 2019; 20: 728.